DISENTANGLING THE MAGNETIC FIELD STRUCTURE OF SUNSPOTS - STEREOSCOPIC POLARIMETRY WITH SOLAR ORBITER

D.A.N. Müller[1], R. Schlichenmaier[2], B. Fleck[1], and G. Fritz[3]

[1] *European Space Agency, Research and Scientific Support Department, c/o NASA Goddard Space Flight Center, Mail Code 612.5, Greenbelt, MD 20771, USA*
[2]*Kiepenheuer-Institut für Sonnenphysik, Schöneckstr. 6, 79104 Freiburg, Germany*
[3]*Arnold Sommerfeld Center for Theoretical Physics, Theresienstr. 37, 80333 München, Germany*

ABSTRACT

Sunspots exhibit complex, highly structured magnetic fields and flows. Disentangling the atmospheric structure of sunspots is a great challenge, and can only be achieved by the combination of spectropolarimetry at high spatial resolution and detailed modeling efforts. We use a generalized 3D model that embeds magnetic flux tubes in a stratified atmosphere and calculates the emerging polarization of spectral lines for arbitrary viewing angles. The resulting polarization maps are a very efficient tool to distinguish between different atmospheric scenarios and determine the 3D structure of the magnetic field and the flow field. In this contribution, we present synthetic maps of the net circular polarization (NCP) as a function of the heliocentric angle for different spectral lines of interest. Among those are the Fe I 617.3 nm line which would be observed by the VIM instrument aboard Solar Orbiter and the Fe I 630.2 nm line which will be observed by Hinode (formerly known as Solar-B).

Key words: Sun: sunspots – Sun: photosphere – Sun: magnetic fields – Sun: atmosphere.

1. INTRODUCTION

Spectral line profiles in the penumbra are characterized by line shifts and line asymmetries of their intensity (Stokes-I) as well as in polarized light (Stokes Q, U, and V). A suitable measure of the asymmetry of Stokes-V profiles is the area asymmetry or *net circular polarization*, $\mathcal{N}$, of a spectral line, which we define as

$$\mathcal{N} \equiv \int_{\delta\lambda} V(\lambda)\,\mathrm{d}\lambda\,, \qquad (1)$$

where the interval of integration, $\delta\lambda$, encompasses the whole line profile. This quantity has the advantage that it is independent of the spatial resolution of the observations since a convolution of a line profile with a Gaussian preserves its area. The first measurements of the net circular polarization in sunspots were reported by Illing et al. (1975), and Auer & Heasley (1978) showed that these observations could be explained by assuming macroscopic velocity fields. Furthermore, they proved that velocity gradients are a necessary *and* sufficient condition to produce a NCP.

The advent of modern polarimeters like the Tenerife Infrared Polarimeter (TIP) and the Polarimetric Littrow Spectrograph (POLIS) at the Vacuum Tower Telescope (VTT) on Tenerife has brought new challenges to observers as well as theoreticians. It is now possible to routinely obtain maps of the full Stokes vector for a whole sunspot. This facilitates the study of spectral signatures of magnetic flux tubes in the penumbra by analysis of maps of the NCP.

So far, the spectral synthesis has been limited to atmospheric models based on snapshots of the moving tube model simulations by Schlichenmaier et al. (1998) and to configurations in a two-dimensional plane ("slab models"). Such slab models have been used earlier by Solanki & Montavon (1993), Sánchez Almeida et al. (1996) and Martínez Pillet (2000) and lead to the picture of the "uncombed" penumbra: Approximately horizontal magnetic flux tubes are embedded in a more inclined background field which is at rest. The sharp gradient or even discontinuity of the velocity of the plasma between the inside the tube and the static surroundings result in the observed NCP. Two-dimensional models succeeded in reproducing the observed NCP and its center-to-limb variation. However, these models are limited to the few geometric cases where a flux tube is exactly aligned with the line-of-sight and do not give any information about the NCP at different positions within the penumbra.

We showed (Müller et al. 2002; Schlichenmaier et al. 2002) that a wealth of additional information is contained in NCP maps that can be retrieved with the help of a three-dimensional model. Jumps in the azimuth of the magnetic field (as measured in the observer's coordinate system) lead to a characteristic pattern of the NCP within the penumbra. Specifically, it was shown that the apparent symmetry within the spot is broken due to the following fact: The jumps in the magnetic field azimuth are

different for two locations which are symmetrically located in the spot with respect to the "line-of-symmetry" (Fig. 1).

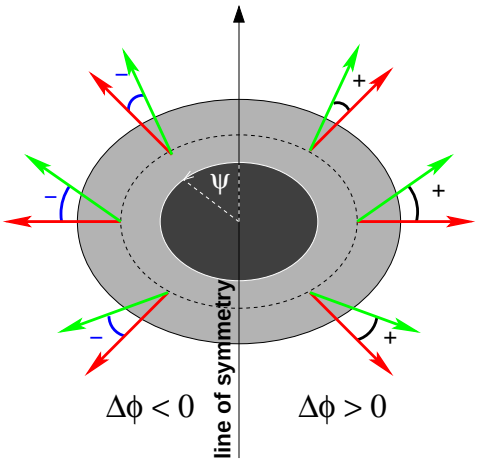

Figure 1. Pictorial representation of the difference in azimuth, $\Delta\phi(\psi)$, between the magnetic field vector inside a flux tube (red arrows) and that of the background field (green arrows). The tubes are nearly horizontal, while the field vector of the background has a steeper inclination, but is also in the plane spanned by the spot axis and the flux tube axis.

The impact of this geometric effect on the NCP strongly varies between spectral lines at different wavelengths. A comparison of the NCP of different spectral lines can thus be used to diagnose the magnetic field inclination and orientation of flow channels in the penumbra.

Furthermore, the NCP varies strongly as a function of the heliocentric angle, θ (Müller et al. 2002), and an analysis of the NCP of the same region for different θ angles is able to reveal details about its atmospheric structure. When one observes sunspots from one viewpoint, however, the heliocentric angle changes only slowly with time as the sunspot moves across the disk. Since the fine structure of sunspots evolves on a much shorter time scale than that of the solar rotation, only a statistical analysis of a set of sunspots at different heliocentric angles may give additional information about the magnetic field configuration. On the other hand, a second vantage point renders stereoscopic polarimetry possible. Analyzing near-simultaneous polarimetric data from two different viewing angles would help to disentangle complex magnetic structures, for example the fine structure in the penumbra, and in general help to resolve the 180° ambiguity in vector magnetic field measurements. The Solar Orbiter will provide such a second vantage point, and we will show how one can distinguish between different atmospheric by detailed forward modeling of the resulting NCP.

2. THE VTUBE MODEL

In order to gain a better understanding of the different factors that determine the NCP and its spatial variation within the penumbra, we constructed a 3D geometric model (VTUBE) of a magnetic flux tube embedded in a background atmosphere. This model serves as the frontend for the radiative transfer code DIAMAG (Grossmann-Doerth 1994). Combining the two, we can generate synthetic NCP maps for any desired axisymmetric magnetic field configuration and arbitrary flux tube properties. The model has been built to offer a high degree of versatility, e.g. the option to calculate several parallel rays along the line-of-sight which intersect the tube at different locations. One can then average over these rays to model observations of flux tubes at different spatial resolutions and for different magnetic filling factors of the atmosphere. Furthermore, we can also take into account radial variations of the physical properties of the flux tube. Doing so, one can e.g. model the interface between the flux tube and its surroundings.

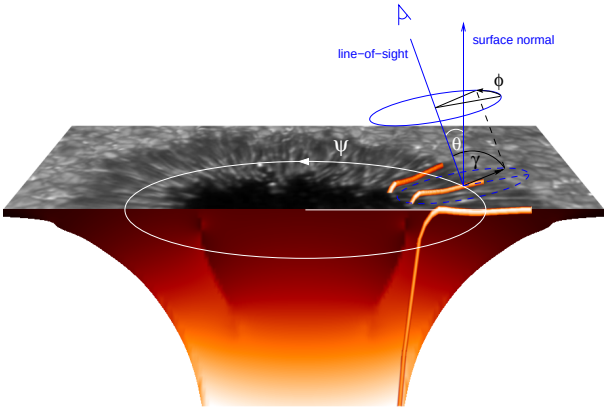

Figure 2. Magnetic flux tubes in the penumbra. For a given heliocentric angle θ, the azimuth ϕ and the inclination γ of the magnetic field vary with the location of the flux tube in the sunspot, characterized by the spot angle ψ.

Figure 2 shows the relevant angles which occur in the model. For a given heliocentric angle θ, the azimuth ϕ and the inclination γ of the magnetic field vary with the location of the flux tube in the sunspot, characterized by the spot angle ψ. The sketch in Fig. 3 additionally shows the tube inclination angle, α. The VTUBE model is described in detail in (Müller et al. 2006). For the calculations presented in this contribution, no averaging over parallel rays was performed, and the physical quantities were kept constant along the flux tube radius (thin flux tube approximation).

2.1. Building a realization of the model

The following steps are performed to assemble a realization of the penumbral flux tube model:

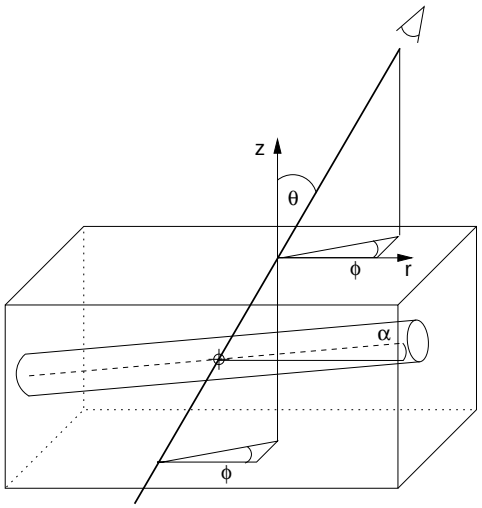

Figure 3. Embedding a flux tube in a background atmosphere. The line-of-sight is defined by the magnetic field's inclination θ and azimuth ϕ. The local inclination of the flux tube is given by the angle α.

1. In the first step, the background magnetic field of the penumbra, $\mathbf{B}(r, z)$, is prescribed.
2. The flux tube axis is defined by a polygon or spline function.
3. The physical properties of the flux tube are defined and then interpolated along the flux tube axis.
4. A functional dependence of the physical properties on the radius of the flux tube can be prescribed, e.g. to model the cooling of a flux tube.
5. The viewing angle is defined by specifying the heliocentric angle and the location of the line-of-sight.
6. The spectral line profiles are calculated.

3. THE ATMOSPHERIC MODEL

For the parameters of the atmospheric background model and the flux tube properties, we use results from two-component Stokes inversions. Analyses of such inversions have demonstrated that two interlaced components are capable of reproducing the spectropolarimetric data sets (cf. Borrero et al. 2006; Bellot Rubio et al. 2004; Beck 2005). The typical properties of these two components are summarized in Fig. 4 and used as input for VTUBE: From the inner to the outer penumbra, the magnetic field strength of the tube component is about 500 G smaller than that of the background component and gradually approaches it as the radial distance from spot center increases. The flow speed increases from 6.5 to 8 km/s in the inner penumbra and stays constant in the outer penumbra. The tube inclination gradually changes from being upwards ($\alpha = 25°$) to downwards ($\alpha = -10°$), with α being measured relative to the horizontal. Assuming that these parameters are axially symmetric, we employed the VTUBE model to calculate synthetic spectra for different viewing angles for the entire spot. For the background atmosphere, we used the penumbra model of Bellot Rubio et al. (2006), and the tube was placed 50 km above optical depth unity with a magnetic flux of 5×10^{16} Mx.

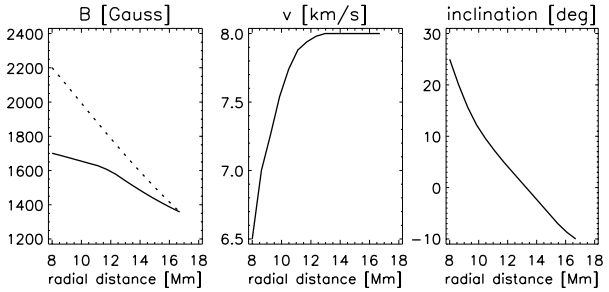

Figure 4. Radial dependence of flow and magnetic field of the two components. These values are used to construct the NCP maps in Fig. 6. The left panel shows the radial variation of the magnetic field strength of the strong background (dotted line) and weak tube (solid line) component. The middle and right panels display the flow speed and the inclination of the tube component relative to the horizontal.

4. RADIAL AND AZIMUTHAL VARIATION OF THE NCP

In a recent article (Müller et al. 2006) we compared the new VTUBE model to the old model used in Müller et al. (2002) and demonstrated the enhanced versatility of VTUBE. One question that we addressed was whether magnetic flux tubes dive back down into lower atmospheric layers in the outer penumbra and, if so, at which angle. Figure 5 (adopted from Müller et al. 2006) shows the variation of the NCP along a circular cut in the outer penumbra for the infrared line Fe I 1564.8 nm. For tube inclination angles of $\alpha \geq -15°$, the curve has two pronounced maxima and minima, while there is only one of each for smaller angles, i.e. more vertical downflows. There are two points to be made here. The first one is that the different shapes of the curves can be explained by applying the simplified analytical model of Landolfi & Landi Degl'Innocenti (1996, see Müller et al. (2002) for details). The NCP is proportional to $-v_{LOS} \cdot \sin(2\Delta\phi)$ where v_{LOS} is the line-of-sight velocity and $\Delta\phi$ is the jump in the azimuth of the magnetic field between the flux tube and the background atmosphere. The second point is that the observed azimuthal variations of the NCP in the infrared line always show two maxima and two minima. This rules out flux tubes that descend at an angle steeper than about $\alpha < -15°$.

These first results were very promising and have stimulated further modeling. Figure 6 shows synthetic NCP

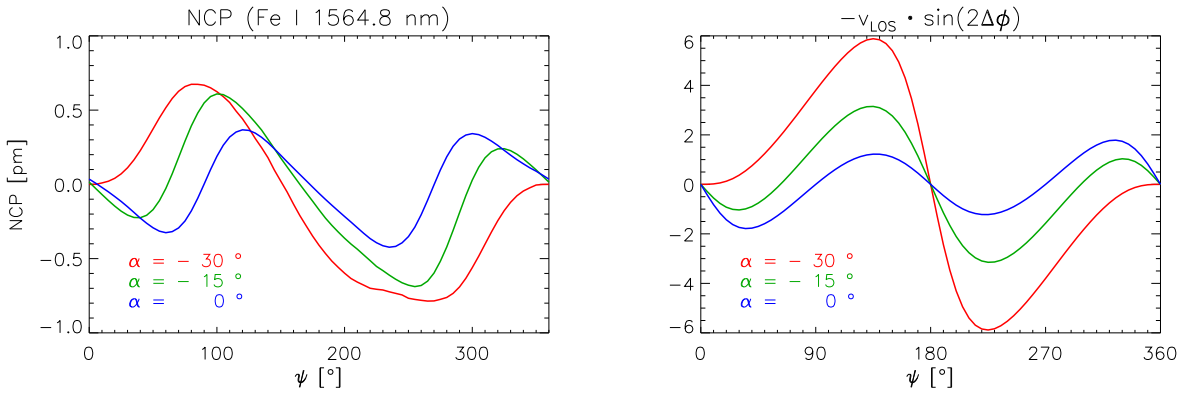

Figure 5. Variation of the NCP along a circular cut in the outer penumbra for the infrared line Fe I 1564.8 nm. For tube inclination angles of $\alpha \geq -15°$, the curve has two pronounced maxima and minima, while there is only one of each for smaller angles, i.e. more vertical downflows. The different shapes of the curves can be approximated by the term $-v_{LOS} \cdot \sin(2\Delta\phi)$ where v_{LOS} is the line-of-sight velocity and $\Delta\phi$ is the jump in the azimuth of the magnetic field between the flux tube and the background atmosphere.

maps for three different spectral lines: Fe I 1564.8 nm (left column), Fe I 630.2 nm (middle column), and Fe I 617.3 nm (right column). While the first two lines have already been studied extensively before, the Fe I 617.3 nm is of particular interest since it would be observed by the VIM instrument on Solar Orbiter. For the background atmosphere we used again the penumbra model of Bellot Rubio et al. (2006), and the flux tube properties are those sketched in Fig. 4.

The Fe I 1564.8 nm line is formed in the lower photosphere and thus shows a clear signature of the rising flux tubes in the inner penumbra. It can also be seen that the NCP distribution has a strong antisymmetric component in the infrared which becomes dominant at large heliocentric angles, while the symmetric component dominates for the NCP of the two visible lines. This is due to the different wavelength dependence of the Doppler effect (linear in λ) and the Zeeman effect (quadratic in λ) and is explained in detail in Müller et al. (2002). The asymmetric feature that becomes visible in the lower right of the Fe I 617.3 nm map at $\theta = 30°$ results from the complex interplay between the $\Delta\phi$ effect and the $\Delta\theta$ contribution of the NCP. The slightly larger NCP of the Fe I 630.2 nm line compared to the Fe I 617.3 nm line in the inner center-side penumbra (red spot in the middle panel of the lower row in Fig. 6) is a result of the higher excitation potential of $\chi = 3.69$ eV of the Fe I 630.2 nm line compared to $\chi = 2.22$ eV for the Fe I 617.3 nm line. In other words, the former line is more sensitive to hotter, i.e. slightly lower layers of the atmosphere where the rising flux tubes are located. Apart from these differences, the maps of both visible lines are similar since the two lines are very similar in wavelength and both have an effective Landé factor of $g_{\rm eff} = 2.5$.

The θ dependence of the NCP was already studied in Müller et al. (2002) for fixed azimuthal positions. With the new VTUBE model, NCP maps for a sequence of heliocentric angles can now be generated routinely. Comparing the different rows of Fig. 6, it becomes clear how strongly the NCP varies as a function of the heliocentric angle θ. Furthermore, the NCP maps are very sensitive to the locations and physical properties of penumbral flux tubes. Simultaneous observations of sunspots from two different θ angles will result in a pair of NCP maps which can then be compared with pairs of NCP maps for different atmospheric scenarios. This will strongly reduce the ambiguity of possible field configurations since only very few, if any, atmospheric configurations will result in the same NCP maps of the penumbra for two different viewing angles. In a future article we will explore the difference between NCP maps for different viewing angles and different atmospheric models.

5. INSTRUMENT REQUIREMENTS FOR SOLAR ORBITER

One of the key advantages of NCP maps is the fact that they contain a large amount of information about the magnetic field in a very small data volume if one has an approximate model of the magnetic field geometry. The Stokes-V profiles at any spatial point are simply integrated, which reduces the data volume by a factor equal to the number of wavelength points at which the spectral line is sampled. In addition to that, the NCP is independent of the spectral resolution. Thus, NCP maps can also be generated from the data of a narrow-band filter imager which is scanned in small wavelength steps across the line. We carried out test calculations and found that a minimum of seven wavelength steps across the Fe I 617.3 nm line is needed to measure the NCP with an accuracy of around 10%.

The first aspect is important for Solar Orbiter since limited telemetry will be a major restriction of this encounter mission. The second one takes into account that the Solar Orbiter will probably not carry a spectropolarimeter, only

a polarimetric filter imager. However, if its polarimetric accuracy is sufficiently high (preferably on the order of 10^{-3}) and the filter can be scanned in sufficiently small steps across the line, a detailed analysis of the magnetic field structure using NCP maps will be possible.

6. SUMMARY

We have presented synthetic NCP maps of a model sunspot penumbra and showed how NCP maps from different viewing angles, for example a ground-based telescope and the Solar Orbiter, can be used to distinguish between different atmospheric configurations. For this work, we used a generalized geometrical model that embeds an arbitrarily shaped flux tube in a stratified magnetized atmosphere. The new model is a versatile tool to calculate the spectral signature of flux tubes in the penumbra and especially make predictions about the flow speed and tube inclination from observed maps of the NCP. We described the instrumental requirements for this type of observations and highlighted the fact that recording NCP maps is an interesting option to study magnetic fields whenever the telemetry rate is restricted and an approximate geometric model of the magnetic field is available.

REFERENCES

Auer, L. H. & Heasley, J. N. 1978, *A&A*, 64, 67

Beck, C. 2005, PhD thesis, University of Freiburg, http://www.kis.uni-freiburg.de/beck_diss.pdf

Bellot Rubio, L. R., Balthasar, H., & Collados, M. 2004, *A&A*, 427, 319

Bellot Rubio, L. R., Schlichenmaier, R., & Tritschler, A. 2006, *A&A*, 453, 1117

Borrero, J. M., Solanki, S. K., Lagg, A., Socas-Navarro, H., & Lites, B. 2006, *A&A*, 450, 383

Grossmann-Doerth, U. 1994, *A&A*, 285, 1012

Illing, R. M. E., Landman, D. A., & Mickey, D. L. 1975, *A&A*, 41, 183

Landolfi, M. & Landi Degl'Innocenti, E. 1996, *Sol. Phys.*, 164, 191

Müller, D. A. N., Schlichenmaier, R., Fritz, G., & Beck, C. 2006, *A&A*, *in press*

Martínez Pillet, V. 2000, *A&A*, 361, 734

Müller, D. A. N., Schlichenmaier, R., Steiner, O., & Stix, M. 2002, *A&A*, 393, 305

Sánchez Almeida, J., Landi Degl'Innocenti, E., Martínez Pillet, V., & Lites, B. W. 1996, *ApJ*, 466, 537

Schlichenmaier, R., Jahn, K., & Schmidt, H. U. 1998, *A&A*, 337, 897

Schlichenmaier, R., Müller, D. A. N., Steiner, O., & Stix, M. 2002, *A&A*, 381, L77

Solanki, S. K. & Montavon, C. A. P. 1993, *A&A*, 275, 283

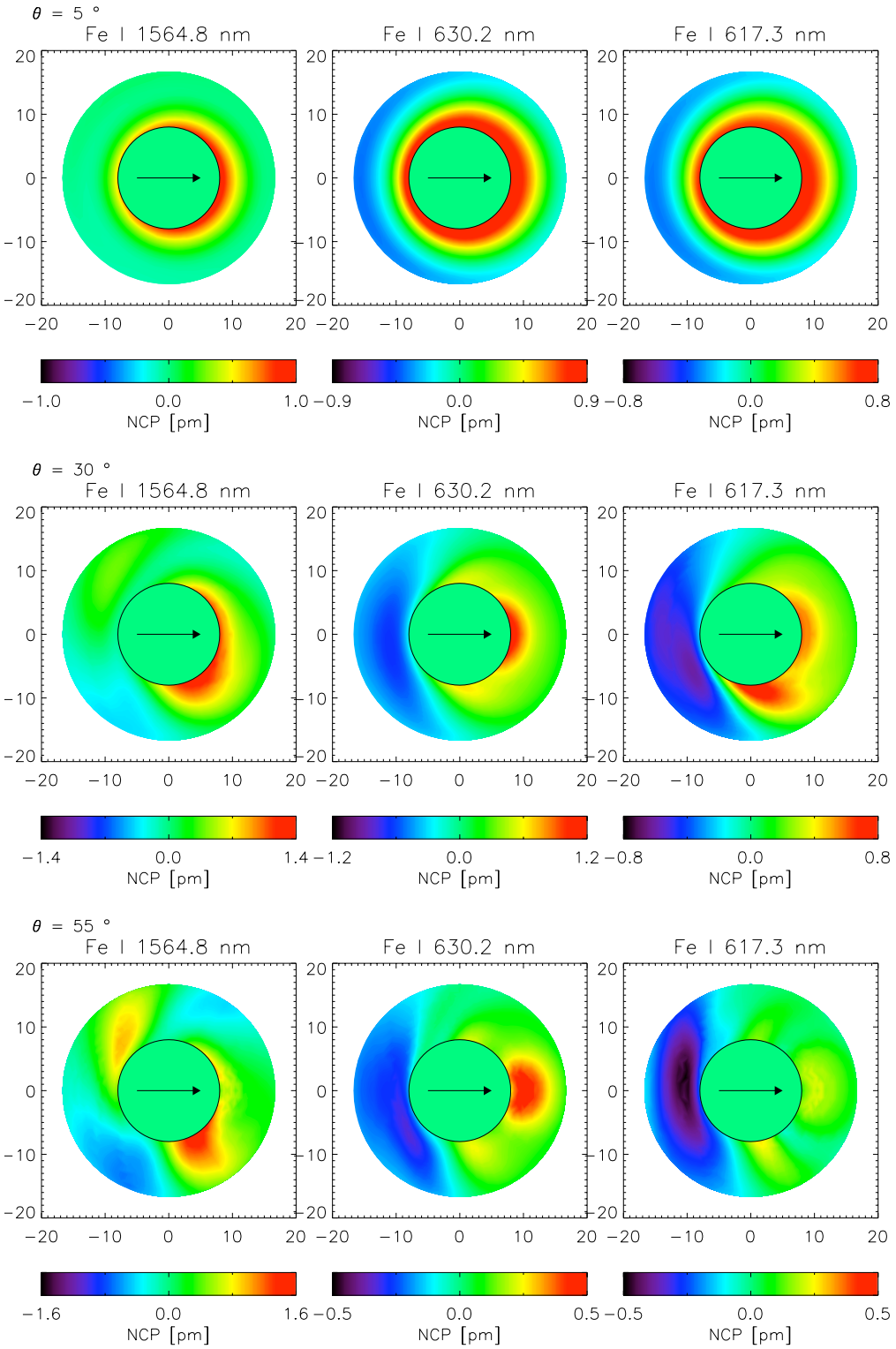

Figure 6. NCP maps for three different spectral lines and for three different heliocentric angles $theta$. Left column: Fe I 1564.8 nm, middle column: Fe I 630.2 nm, right column: Fe I 617.3 nm. Top row: $\theta = 5°$, central row: $\theta = 30°$, bottom row: $\theta = 55°$. In the infrared, the NCP distribution has a strong antisymmetric component which becomes dominant at large heliocentric angles, while the symmetric component dominates for the NCP of the visible lines.